Optovoltaic detection: A new probe for laser spectroscopy

J. R. Brandenberger
Department of Physics, Lawrence University, Appleton, Wisconsin 54912
(Received 15 September 1986)

A krypton discharge fitted with internal ohmic electrodes, excited by external rf electrodes, and perturbed by laser radiation at 785.5 nm, shows a strong optovoltaic signal that differs substantially from the conventional optogalvanic effect. The salient features of the discharge and the major characteristics of the optovoltaic signals are explored spectroscopically using a tunable diode laser that scans the $1s_3 \rightarrow 2p_3$ transition in krypton. Possible mechanisms and applications for this new type of signal are discussed.

I. INTRODUCTION

Optogalvanic detection provides laser spectroscopy with a powerful probe for investigating atoms and molecules in discharge environments.[1] Several different mechanisms have been employed to model optogalvanic detection theoretically,[2–4] but the effect usually manifests itself experimentally as a light-induced change in the impedance of a discharge.[5] This paper describes an experimental setup that produces a different type of response—an optovoltaic rather than optogalvanic one. More specifically, our signals appear as optically induced emf's rather than changes in impedance. Although this new type of signal is largely a creation of our particular setup, its existence and strength are striking. From a practical standpoint, our layout with its attendant optovoltaic signal offers the notable features of high sensitivity, excellent signal-to-noise ratio, and the prospect for minimizing collisional effects within the discharge environment. In the following discussion we concentrate upon the characteristics of our discharge and the optovoltaic line shapes that we observe in a krypton cell scanned by a tunable diode laser.

II. EXPERIMENTAL PROCEDURE

Discharge cells suitable for the exploration of optovoltaic signals can be removed from commercially available spectral lamps.[6] We excite such cells with a 30-MHz oscillator[7] coupled to the discharge through a pair of external ring-shaped electrodes as shown in Fig. 1. This system provides weak albeit stable excitation with rf voltages of only 30 V and rf fields of roughly 20 V/cm. Through loading measurements, we infer that the nominal rf power absorbed by the discharge is 15 mW and that the rf currents approach 1 mA. Since our cell contains 5 Torr of natural krypton, the atomic density is $\simeq 10^{17}$ cm^{-3}. Combining these figures with an electron-krypton collision cross section of 3×10^{-16} cm^2, we estimate an electron-atom collision rate of 9 GHz, an electron mobility of 20 m^2/V sec, and an electron density of 10^{10} cm^{-3} in the luminous region of the discharge. Assuming an electron temperature of 5–10 eV, the predicted Debye length of 0.2 mm suggests that we have a "glow" discharge whose properties approach that of a plasma.

The optovoltaic signal of interest here stems from laser excitation of the 785.5-nm $1s_3 \rightarrow 2p_3$ transition in krypton. Metastability in the $1s$ manifold is important because it insures large $1s_3$ and $1s_5$ populations in our discharge cell. To verify this claim, we pass a 785.5-nm laser beam through the faintly luminous krypton discharge. As the laser approaches the $1s_3 \rightarrow 2p_3$ transition, 557.0-nm fluorescence indicative of $2p_3 \rightarrow 1s_5$ relaxation becomes visible within the narrow 3-mW laser beam. When the laser is tuned to line center, this fluorescence increases dramatically and envelops a large fraction of the discharge. This behavior indicates multiple scattering and suggests that the 557.0-nm radiation inside the discharge has an absorption length of roughly 1 cm. One can use this number to estimate the density of $1s_5$ metastable atoms (the reabsorbers in this case) using[8]

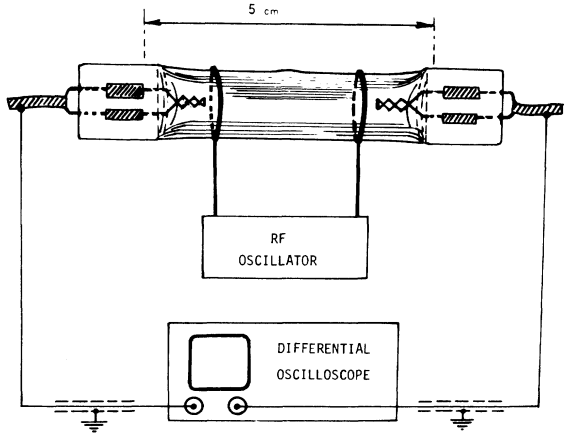

FIG. 1. Simple krypton cell used in this work. The external ring-shaped electrodes provide rf excitation of the discharge while the ohmic electrodes at opposite ends of the cell probe the optovoltaic signal. The rf oscillator has a balanced output and the oscilloscope is differential. An output signal from the oscilloscope drives an X-Y recorder.

$$N(1s_5)=(2\pi kT/m)^{1/2}\frac{8\pi k_0}{(2J+1)\lambda^3\gamma}\ , \tag{1}$$

where $J=1$ pertains to the $2p_3$ state, $\lambda=557.0$ nm, $k_0=1$ cm^{-1}, and γ is the $2p_3\rightarrow 1s_5$ transition probability. The result is $N(1s_5)=10^{13}$ metastable atoms/cm^3; presumably the $1s_3$ population is similarly large.

The remaining constituent is Kr^+. To assure approximate neutrality in the luminous region, the Kr^+ density there should match the aforementioned electron density of 10^{10} cm^{-3}. A Kr^+ density this small agrees with our failure to detect any Kr II lines in the otherwise strong Kr emission emanating from our cell. This absence of a Kr II spectrum suggests that the Kr^+ population is several orders of magnitude smaller than the Kr population lying above the $1s$ manifold. If one estimates the latter to be comparable to the 10^{13} metastable atoms/cm^3 known to lie in the $1s$ manifold, one arrives again at a Kr^+ density on the order of 10^{10} cm^{-3}. Such a low Kr^+ density also squares with our small E/p ratio of 4 V/cm Torr, although more relevant to the present case of rf excitation is the ratio of electron collision rate to rf frequency.

The work reported here involves a 5-mW cw single-mode $Al_xGa_{1-x}As$ diode laser[9] which scans the 785.5-nm line of Kr. Temperature stabilization and current regulation for the diode resemble an approach developed elsewhere.[10] The most distinctive features of this work stem from rf excitation and the use of a pair of ohmic electrodes which pass through the ends of the cell to pick up the optovoltaic signal. These electrodes couple directly to 1-MΩ inputs on a differential oscilloscope which drives a recorder. Chopping and synchronous detection are unnecessary due to the quietude of the discharge and stability of the laser.

The discharge is composed of a cigar-shaped glow region which resembles a positive column in a dc discharge.[11] A 2-mm-thick dark space or ion sheath surrounds the glow and isolates it from the walls of the cell. At low rf levels, the glow occupies about half the space between the rf electrodes, while at high rf levels it extends all the way to the ohmic electrodes. Excitation by external electrodes and ambipolar diffusion of the electrons and ions are conjoined by an accumulation of negative charge on the inner walls of the cell.[12] This condition stems from the following: (i) in the steady state the time-averaged total current arriving at the walls must be zero because the walls are nonconducting, and (ii) the surface charge must be sufficiently negative to repel a large fraction of the highly mobile electrons that would otherwise move toward the walls during alternate half cycles of the rf excitation. The dark space or sheath assumes a positive charge because it contains Kr^+ and neutrals, the electrons having been largely repelled by the negative walls. We surmise that the electric fields in the sheath are mainly radial (extending outward from the Kr^+ ions to the negative walls) and comparable in strength to the peak rf fields.

The situation is different at the ends of the cell where the sheath wraps around the glow and shrouds the ohmic electrodes in darkness. Surrounded mainly by ions, metastables and ground-state atoms, the metallic electrodes play a critical role by providing the metastable atoms with a deactivation surface. In our case of metastable Kr impinging upon tungsten electrodes, deactivation is frequently accompanied by the ejection of an electron from the electrode. Hence metastable deactivation provides a mechanism whereby the ohmic electrodes eject electrons *into* the discharge. The electrodes thus behave as if they contain current sources or emf's whose negative terminals face the discharge and whose positive ports point outside the cell. If the laser is off or detuned and the discharge is symmetric relative to the ohmic electrodes, equal rates of deactivation and electron ejection will take place at both electrodes. In this case, the current sources or emf's cancel each other, and no net current flows through the external circuit. If, however, a 785.5-nm laser beam passing near electrode A depletes the local $1s_3$ population via optical pumping to the $2p_3$ state, then the symmetry is broken. The result is a diminished ejection rate at electrode A, which in turn lets the ejection rate at electrode B dominate. It follows that electrons will flow around the *external* circuit from electrode A to electrode B precisely as we observe.

III. OPTOVOLTAIC LINE SHAPE

Now we discuss the optovoltaic line shape; our objective is to identify its salient features and pave the way for further discussion of the origin of the optovoltaic signal. We stress that the signals observed here represent emf's—there is no external bias as in the conventional optogalvanic case. Through careful positioning of the rf electrodes while the laser is detuned, we null the voltage between the ohmic electrodes, thereby establishing discharge symmetry and an optovoltaic baseline of zero volts. Then when the laser is tuned to resonance, one observes hundreds of millivolts of optovoltaic signal whose magnitude and polarity depend upon laser power, discharge conditions, and beam placement. Although we vary the location of the laser beam within the cell, it always intersects the cylindrical axis orthogonally.

Figure 2 exhibits the major features of the line shape and shows the effects of attenuating the laser beam with neutral density filters. The stick diagram identifies the contributions from ^{83}Kr (12% abundance) and ^{82}Kr, ^{84}Kr, and ^{86}Kr (86% collective abundance). These line shapes suggest a ^{83}Kr hyperfine structure (hfs) splitting of 2.3(1) GHz in agreement with Jackson's 2.262(6) GHz.[13] Marginal resolution here is due to collisional effects and Doppler broadening, which we expect to reduce in the future. The satellites riding on the wings of the resonance are replicas of the central resonance excited by laser sidebands whose power is typically 1% of the power of the principal mode. When the differences in laser power for the various features in this line shape are taken into account, one finds that all five features scale with laser power in roughly the same manner.

Figure 3 shows the dependence of the optovoltaic signal upon rf level. For low rf levels, the signal scales linearly with rf absorption. In the case shown here, for which the laser power of 5 mW is abnormally high, saturation sets in at only 4 mW of rf absorption, and broadening is evident at high rf power. These optovoltaic signals resemble

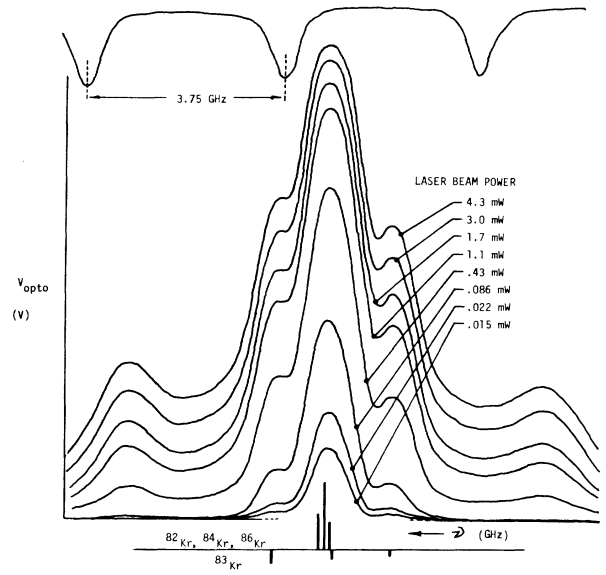

FIG. 2. Optovoltaic signal V_{opto} vs laser frequency ν for various laser-beam powers. The 785.5-nm laser beam passes along the edge of the glow region. The outermost features on the line shape are replicas of the central resonance driven by laser sidebands. The stick diagram identifies the hfs contribution from ^{83}Kr and the unresolved contributions from ^{82}Kr, ^{84}Kr, and ^{86}Kr. The Fabry-Perot scan at the top calibrates the horizontal scale.

fluorescent line shapes, which we acquire occasionally, but saturation is much more prevalant in the optovoltaic case. Since saturation tends to discriminate against major features in a line shape, the result is a relative accentuation of minor components. This is the reason why the sideband driven replicas are so pronounced in many of these line shapes. Some of the changes in the resonances shown in Fig. 3 are due to elongation of the glow region as the rf level is raised (see discussion below in conjunction with Fig. 5).

The line shapes shown in Fig. 4 reveal the effects of increasing the laser power (neutral density filters are not used here) at a constant rf level. Most striking is the outward shift of the replicas as the laser power increases. The laser sidebands that drive these spectral replicas are traceable to relaxation oscillations within the laser. The shifting of the replicas agrees with the known property[14] that the splitting $\Delta\nu$ of the sidebands from the principal mode of the laser scales as (laser power)$^{1/2}$. The sideband powers tend to be unequal, the lower frequency sideband often being 15% more powerful.[15] It follows that if one scans in the direction of increasing laser frequency, the stronger replica (driven as it is by the stronger but lower frequency sideband) occurs at a frequency above the central resonance as observed in Fig. 4.

The line shapes shown in Fig. 5 reveal that as the 2-mm-diam laser beam is swept from one ohmic electrode to the center of the cell, the optovoltaic signal undergoes change in both strength, shape, and polarity. Noteworthy here are the following: (i) the signal attains maximum strength when the beam strikes the edge of the glow (where, presumably, the $1s_3$ population is greatest), (ii) if the glow is sufficiently long, the polarity of the signal reverses as the laser beam approaches the center of the discharge, and (iii) the signal disappears when the laser beam passes through the center of the discharge (at this point the laser cannot disrupt the symmetry).

IV. DISCUSSION

We believe that these optovoltaic signals stem from an asymmetric optically induced redistribution of $1s$ krypton atoms in the vicinity of the ohmic electrodes. Defining the "selected electrode" as that ohmic electrode to which the laser beam is closer, we argue that optical depletion of the $1s_3$ metastable atoms near the selected electrode reduces the deactivation-induced electron ejection at the

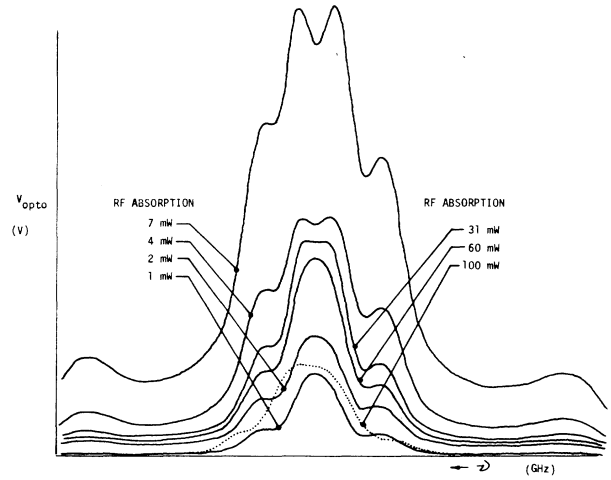

FIG. 3. Optovoltaic signal V_{opto} vs laser frequency for various levels of rf absorption. Abnormally high laser power of 5 mW accentuates saturation and produces dips at tops of several line shapes.

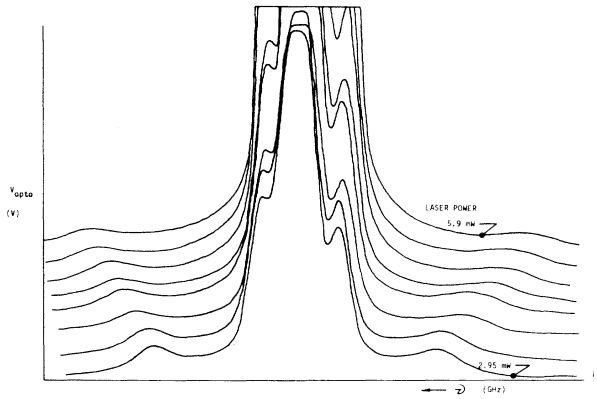

FIG. 4. Optovoltaic signal V_{opto} vs laser frequency for various laser powers ranging from 5.9 (upper trace) to 2.95 mW (lower trace). With increasing laser power, the sideband-driven replicas of the central resonance shift outward.

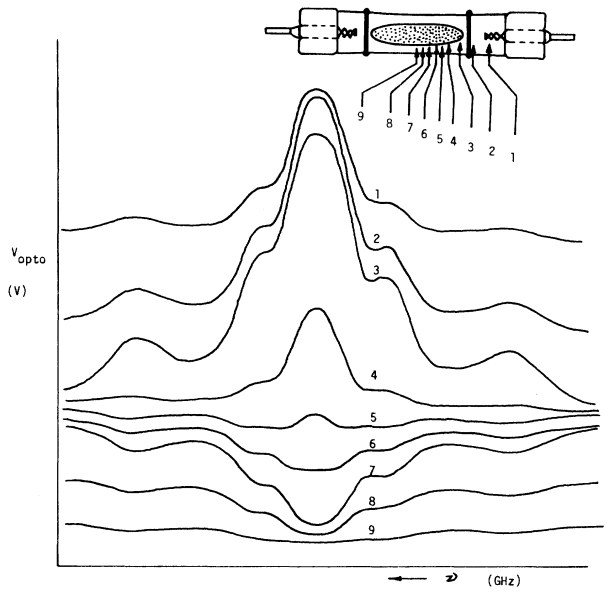

FIG. 5. Optovoltaic signal V_{opto} vs laser frequency for nine different laser-beam locations relative to luminous portion of krypton discharge. Laser beam diameter is 2 mm; laser power is 3 mW; rf absorption is 15 mW. Baselines have been shifted to minimize confusion.

selected electrode. Given a previously balanced or symmetric discharge, the optical resonance reduces the ejection rate at the selected electrode and breaks the symmetry, thereby passing ejection rate dominance to the nonselected electrode. The result is a net electron current that is drawn out of the selected electrode, drawn through the external circuit, and drawn back into the discharge by way of the dominant nonselected electrode.

A reduction in the $1s_3$ metastable population due to $1s_3 \rightarrow 2p_3$ pumping at 785.5 nm is in fact expected because the branching ratio from the $2p_3$ state admits a 36% chance of decay to the $1s_2$ state, which is strongly resonant with the $^1p_0$ ground state. While light trapping will lengthen the lifetime of the $1s_2$ state, this state will nevertheless offer an effective sink for $2s_3$ metastable atoms which undergo excitation to the $2p_3$ state.

As shown in Fig. 5, the polarity of the optovoltaic signal is invariant to a repositioning of the laser beam so long as it falls within a zone bounded by one ohmic electrode and a plane lying roughly one-third of the way into the glow region. This zone encompasses three distinctly different situations whereby the laser beam interacts with atoms amidst, close to, or fairly distant from the selected electrode. In discharge terms, these interactions lie deep in the sheath, near the sheath-glow interface, or part of the way into the glow region, respectively. Under these conditions, the optovoltaic signal always exhibits the same polarity, a polarity which is consistent with electrons flowing out of the selected electrode, through an external load, and back into the discharge via the nonselected electrode. In other words, the selected electrode has the lower electrostatic potential. In most cases the external load is the 2 MΩ presented by the differential oscilloscope.

Our conviction that this 785.5-nm optovoltaic signal is traceable to the depopulation of the $1s_3$ metastable atoms rather than to impact ionization of $2p_3$ krypton atoms by metastable atoms or electrons, is based upon a simple calculation[16] which shows that the $2p_3$ state, with its lifetime of only 23 nsec, cannot contribute significant amounts of ionization in the present discharge. One finds that the rate of $2p_3$ impact ionization due to collisions with metastable atoms in our discharge is 10^{-4} less than the spontaneous decay rate of the $2p_3$ state. The ionization rate of the $2p_3$ state due to electron impact is only slightly larger. These figures strongly suggest that the optovoltaic signal in a discharge as weak as the present one must involve the $1s_3$ state directly; no significantly populated higher-lying states live long enough to produce such a large effect.

This identification of the source of our signal is strengthened by the following consideration. For reasonably strong optovoltaic signals of 200 mV or so, corresponding to a net external current of 0.1 μA, we find that the $1s_3$ metastable atoms absorb about 1 μW from the 2-mW 785.5-nm laser beam passing through the cell. These figures are in excellent agreement if one allows for the 36% branching probability for the $2p_3 \rightarrow 1s_2$ transition (which sinks the optically pumped metastables) and assumes an electron ejection efficiency of 50% for $1s_3$ metastable atoms deactivated by tungsten electrodes.

Photoionization is not a probable cause of this signal. To verify this assertion, we subject the discharge and its electrodes to 5 mW of 633-nm laser light and 100 W of light from a Hg arc. No additional optovoltaic signal is observed, thereby confirming that photoionization plays no role in this resonant effect.

Further support for the contention that the optovoltaic signal is traceable to deactivation of $1s_3$ metastable atoms comes from a subsidiary experiment in which an external bias and ballast resistor are wired in series with the ohmic electrodes, as in the conventional optogalvanic configuration. rf excitation is retained, but varying degrees of rf and dc excitation are employed so that one can "situate" the experiment anywhere between the optovoltaic and optogalvanic extremes. This work reveals that when the system is operated optogalvanically (using mostly dc excitation), the cell shows the expected resonant increase in impedance due to laser-induced depletion of the $1s_3$ metastable state, recognizing as we have all along that the $1s_3$ state is a major sustainer of the discharge. When, however, the dc bias is reduced and the rf excitation is increased to the point where the latter becomes dominant, the cell exhibits a resonant decrease in impedance, suggesting an increase in charge density. We attribute this increase in charge density to the aforementioned mechanism, namely to the net current that results from imbalanced metastable deactivation at the ohmic electrodes.

It is difficult to think of other processes that would produce signals of the observed polarity. Take for instance the hypothetical case of photoejection of electrons from an ohmic electrode due to a laser-triggered cascade of uv photons. This process would produce a signal of the wrong polarity. Another possible mechanism might arise

from a decrease in the Kr^+-e^- recombination rate at an ohmic electrode due to laser depletion of $1s_3$ metastables nearby. Mobility considerations rule out this mechanism: any decrease in the Kr^+ density due to a decrease in the $1s_3$ population would be accompanied by an equal decrease in the electron density in the same region. Since the electron's mobility is much greater, the electron density will show evidence of change far more quickly and widely (the massive Kr^+ ions will remain essentially stationary by comparison). In this case, the hypothetical decrease in both Kr^+ and electron densities will produce a signal of the wrong polarity.

A final mechanism that has been discussed in recent years[4] concerns the transfer of energy from a laser beam to an electron gas by way of atomic absorption followed by superelastic collisions with electrons. The electron gas is thereby heated, thus leading to a decrease in the impedance of the discharge. This mechanism appears to have merit if one considers the glow region exclusively, but we observe strong optovoltaic signals even when the laser illuminates the dark region. Since this region is electron starved, it does not provide an environment that can support this mechanism.

We conclude this section with a discussion of whether the proposed model accounts for the features of the optovoltaic line shapes presented in Sec. III. Taking Fig. 5 first, we see that the observed polarity of the signal, the observed invariance of signal polarity within a wide zone, and the observed disappearance of the signal are consistent with the model. The cause of the reversal in polarity is not clear at present. The line shapes of Figs. 2–4 are in good accord with the model.

V. CONCLUSION

We close by raising the question is the optovoltaic effect really different from the conventional optogalvanic effect? Though the physics is much the same, we feel that there are differences. This paper has already dealt with several of them, most of which arise from the use of electrodeless rf excitation in conjunction with signal sampling by ohmic electrodes. Here we underscore some additional differences.

We begin by repeating that the baseline for the optovoltaic signal is zero. In the case of weak signals, this situation is preferable to the optogalvanic case in which there is always a quiescent current passing through the discharge, a current that is usually much larger than the signal current. A second difference is that rf discharges are usually quieter than dc discharges; it follows that optovoltaic detection is less likely to suffer limitation due to discharge noise and instability. Thirdly, rf discharges can be sustained at much lower pressures with significantly lower currents; it follows that spectroscopic work should benefit from optovoltaic rather than optogalvanic detection. A fourth point concerns sensitivity: with considerable effort in search of optimum conditions, Keller and Zalewski[4] attained an optogalvanic detection sensitivity of about one signal electron for every ten 614.3-nm photons absorbed in a neon discharge of 5 Torr. Our experimental situation is similar, and our nonoptimized sensitivity is one signal electron for every thirty 785.5-nm photons absorbed by krypton. Although our sensitivity would appear to be $\frac{1}{3}$ that of Keller and Zalewski, the two are probably on a par since the 614.3-nm transition in neon is ten times stronger than the 785.5-nm transition in krypton. Finally, we remind the reader that the signal-to-noise ratio in our signal is sufficiently large to obviate the need for chopping and synchronous detection; rarely is this the case in conventional optogalvanic work.

ACKNOWLEDGMENTS

This work was supported by Research Corporation and Lawrence University. It is a pleasure to acknowledge the valuable assistance of LeRoy Frahm and Harold Everson in the development of instrumentation for this work.

[1]J. E. M. Goldsmith and J. E. Lawler, Contemp. Phys. **22**, 235 (1981).
[2]J. E. Lawler, Phys. Rev. A **22**, 1025 (1980).
[3]C. R. Webster and R. T. Menzias, J. Chem. Phys. **78**, 2121 (1983).
[4]R. A. Keller and E. F. Zalewski, Appl. Opt. **19**, 3301 (1980).
[5]C. Stanciulescu *et al.*, Appl. Phys. Lett. **37**, 888 (1980).
[6]Our cell was removed from a Philips 93101E spectral lamp by carefully cracking and gently crushing the outer glass envelope. With the cutting of two leads, the inner Kr-filled cell is free and ready for use.
[7]W. E. Bell, A. L. Bloom, and J. Lynch, Rev. Sci. Instrum. **32**, 688 (1961).
[8]C. G. Carrington, J. Phys. B **5**, 1572 (1972).
[9]We use Sharp LT026MD and Mitsubishi ML 4102 diode lasers.
[10]The diode controller employed here consists of three circuits: two employ separate thermistor bridges to sense and regulate (by heating and/or cooling) the temperature at two locations in the laser head using Peltier devices. The third circuit monitors, regulates, and facilitates sweeping of the diode current. These circuits were developed by S. K. Lamoreaux and others in the Department of Physics, University of Washington, Seattle, Washington. The present author has been advised that the entire controller will be described in detail in a forthcoming paper.
[11]G. Francis, *Ionization Phenomena in Gases* (Butterworths, London, 1960).
[12]H. S. Butler and G. S. Kino, Phys. Fluids **6**, 1346 (1963).
[13]D. A. Jackson, J. Opt. Soc. Am. **67**, 1638 (1977).
[14]K. Y. Lau and A. Yariv, IEEE J. Quantum Electron **QE-21**, 121 (1985).
[15]K. Vahala, Ch. Harder, and A. Yariv, Appl. Phys. Lett. **42**, 211 (1983).
[16]J. E. Lawler (private communication).